PREPARATION OF SILVER NANOPLATES FOR ANTIBACTERIAL APPLICATION

Trinh Nhu Bao[1,2], Nguyen Anh Thu[1,2], Phan Thi Ngoc Cam[1,2], Truong Tan Trung[3], Vo Khuong Quoc[1,2*]

[1]*University of Science, Vietnam National University - Ho Chi Minh City*
[2]*Vietnam National University - Ho Chi Minh City*
[3]*Dong Nai Technology University*
*Corresponding author: *Khuong Quoc Vo, vqkhuong@hcmus.edu.vn*

GENERAL INFORMATION

Received date: 14/12/2023

Revised date: 02/03/2024

Published date: 12/03/2024

KEYWORD

Anti-bacterial activity of silver nanoplates;

Silver nanoplates.

ABSTRACT

Silver nanoplates (AgNPls) are attractive due to their unique properties, including localized surface plasmon resonance (LSPR) and antibacterial ability due to their vicinity tips and edges. This study reports a rapid and facile methodology for preparing Ag nanoplates using a single-step synthesis approach with the presence of $AgNO_3$ precursor, $NaBH_4$, TSC, and an oxidation agent H_2O_2. Adjusting precursor ratios can yield various morphologies such as spherical, nanodisks, hexagonal structures, and triangular nanoplates, each exhibiting different LSPR. The optical properties of AgNPs were analyzed using UV-Vis spectroscopy and supported by SEM morphology analysis. The crystal strutures were characterized by TEM, and HR-TEM. Furthermore, the anti-bacterial activity was also evaluated against four bacterial strains, including *Staphylococcus aureus, Listeria innocua, Escherichia coli,* and *Pseudomonas aeruginosa*. The AgNPLs prepared in this study exhibited better antibacterial activity against Gram-positive bacteria at low concentrations (0.625 µg/mL) than Gram-negative bacteria.

1. INTRODUCTION

Along with the continuous development of nanotechnology, silver nanoparticles (SNPs) have continuously attracted the attention of researchers in many fields in recent years, including surface-enhanced Raman scattering (SERS) (Munro et al., 1995), analysis (Furletov et al., 2023), and antibacterial (Lu et al., 2015). Among different shapes of SNPs, silver nanoplates (AgNPls) have attracted much attention due to their intrinsic morphology, which is involved in the thinness of plates or truncation of the tips. The synthesis process of silver nanoplates (TSNPs) with many modifications for tuning the shape and size of the final nanomaterials' properties is of great interest (Amirjani et al., 2019). The asymmetry of silver nanoplates will exhibit more LSPR bands than the spherical form. The maximum LSPR wavelength of silver nanoplates can be controlled in the visible and near-infrared regions depending on the shape, size, and edge length. Silver nanoparticles can be precisely synthesized to control their shape and size to govern their optical properties (Djafari et al., 2019).

Silver nanoparticles (AgNPs) have gained lots of attention due to the continuous upsurge in antibacterial applications (Anees Ahmad et al., 2020; Guzman et al., 2012). The antimicrobial effects of AgNPs are supposed to be associated with four defined mechanisms: (1) adherence of AgNPs to the cell wall and membrane surface, (2) penetration of AgNPs into the cell, resulting in damage to intracellular structures such as mitochondria, vacuoles, ribosomes, and biomolecules including proteins, lipids, and DNA , (3) induction of cellular toxicity and oxidative stress through the generation of reactive oxygen species (ROS) and free radicals, and (4) AgNPs modulate cellular signal system, resulting in cell death (Dakal et al., 2016). Many reports indicated that the antibacterial activity of nanomaterials largely depends on their morphology because the Ag^+ ion release capacity changes with their shape (Dong et al., 2019; Fu et al., 2006; Sotiriou et al., 2012). Pal et al. found that anisotropic nanoparticles are more effective at inhibiting bacteria than spherical ones due to their antibacterial properties (Dakal et al., 2016). Therefore, it will be possible to control the antimicrobial activity by developing the unique shape and size of the AgNPs (Cheon et al., 2019). Because silver nanoplates are covered with {111} faces on the surface could interact directly with bacterial cell membranes (Gao et al., 2013). These particles are oxidized to form Ag^+ ions that cross the cell membrane easily, leading to cell death by destroying protein structures. Besides, shape tips of silver nanotriangles with higher surface energy could enhance Ag^+ release ability, increasing antimicrobial effects (Djafari et al., 2019).

However, controlling reagent parameters could be highly challenging, affecting synthesis efficiency, especially in maintaining the nanomorphology and size of silver nanoplates. The oxidation process of silver nanoparticles leading to a transformation of nanoplates is the main issue when oxidation agents are present in reaction colloids. Due to the thermodynamically unfavorable nature of anisotropic nanoparticles, the particles tend to rearrange to achieve a lower surface energy (Pastoriza-Santos et al., 2008).

In this study, AgNPl was rapidly synthesized using a modified single-step method with fewer toxic chemicals. Besides, the role of reagents in the AgNPl synthesis process was explored to clarify the influence of each reagent on AgNPls morphologies. We also evaluated the antibacterial activity against Gram-positive and Gram-negative bacterial strains including *Staphylococcus aureus, Listeria innocua, Escherichia coli,* and *Pseudomonas aeruginosa*, by *in-vitro* agar disk diffusion method. The sensitivity of AgNPls against various bacterial strains at different concentrations was also investigated, revealing that AgNPls are promising materials for antibacterial applications. That shows silver nanoplates are an ideal material for antibacterial applications.

2. METHODOLOGY

2.1. Chemical

Chemicals for controlled synthesis of silver nanoplates were provided by Xilong Scientific (China) such as trisodium citrate dihydrate (TSC, 99.0%), and Hydrogen peroxide (H_2O_2, 30%). Silver nitrate ($AgNO_3$, 99.9%, molecular weight (Mw): 169.87 g/mol) was purchased from Merck (Darmstadt, Germany). Sodium borohydride ($NaBH_4$, 98%) was bought from Scharlau (Spain). Resazurin (Sigma, Aldrich), Iuria Bertani broth (Himadia, India), DMSO (Merck). Deionized (DI) water was used for all reactions.

2.2. Method

The synthesis process of silver nanoplates (AgNPls) is carried out by one-step reduction, through Zhang's protocol with modification (Zhang et al., 2011) . First, 24.75 mL of deionized water was added to a beaker of 50 mL. Then 60 µL of $AgNO_3$ solution 0.05 M, 0.5 mL of trisodium citrate dihydrate solution 0.075 M, and 40 µL of H_2O_2 (30% wt) were sequence added to the beaker under stirring on a magnetic stirrer at a speed of 600 rpm. Afterward, 200 µL of 0.10 M $NaBH_4$ solution was quickly added to ignite the reaction, and the colloidal solution changed from dark yellow to red, purple, and blue, showing the formation of triangular silver nanoparticles.

Table 1. Investigating parameters of reagents used in the silver nanoplate synthesized process.

Experiments	**1**	**2**	**3**
Reagents	**H_2O_2**	**$NaBH_4$**	**TSC**
H_2O_2 (30% v/v, µL)	From 0 to 60	50	50
$NaBH_4$ (0.1 M, µL)	250	From 100 to 250	200
TSC (M, 0.5 mL)	0.075	0.075	From 0.025 to 1.25
$AgNO_3$(0.05 M, µL)	60	60	60

2.3. Characterization

The UV-Vis spectroscopy was performed by using a UV-Vis-NIR-V670 spectroscopy spectrophotometer (JASCO International Co. Ltd, Tokyo, Japan), with a cuvette of 1.0 cm path length, wavelength from 300 to 850 nm, and scanning rate of 400 nm per minute. The morphology of AgNPls was analyzed using a scanning electron microscope using a Quanta FEG 250 at an acceleration voltage of 10.0 kV. The structure of the material, morphology, and size of silver nanoplates were determined by transmission electron microscope (TEM) using a JEM-1400 microscope. The crystal structure of silver nanoplates were analyzed by High-resolution transmission microscopy (HR-TEM) using an FEI Tecnai G2 F20, USA. The AgNPls size and size distribution were determined by ImageJ software by measuring 60 particles in the SEM image.

2.4. Determination of anti-bacterial activity using well diffusion method

The 8-fold AgNPl solution prepared with the optimal condition in this investigation was centrifuged at 12 000 rpm for 15 minutes and washed three times with DI water to remove residual precursors. Afterward, AgNPls were diluted to different concentrations, including 5, 2.5, 1.25, 0.625, and 0.3125 µg/mL.

The antimicrobial activity of silver nanoplates at different concentrations was determined based on the in-vitro agar disk diffusion method (Saubolle et al., 1978). Accordingly, 100 µL of bacterial solution with a density of 10^8 CFU/mL was spread evenly on the agar plate using a sterile glass spreader. Make holes to create agar wells, and gently place the samples into them, and then incubate for 24 hours at 37°C. The control used in this experiment was distilled water, ampicilin was used as the positive control. The diameter of the anti-bacterial rings was measured using a ruler measuring mm.

3. FINDINGS AND DISCUSSION

The reagents used in the preparation process contribute important roles in synthesizing silver nanoplates, including H_2O_2, $NaBH_4$, and TSC (Agnihotri et al., 2014; Zannotti et al., 2020; Zhang et al., 2011). Herein, we evaluated the impact of H_2O_2 (30%) in the volume range from 0 to 60 µL while keeping the remained reagent parameters constant. Similarly, the volume of $NaBH_4$ 0.10 M was changed in the range from 100 to 250 μL; consequently, the effect of TSC was investigated in the concentration range from 0.025 to 0.125 M. From this study, the appropriate reagent parameters were determined to achieve silver nanoplates with high uniformity and vicinity tips and edges to improve the antibacterial activity.

3.1. Effect of H_2O_2 volume on the formation of AgNPls.

Hydrogen peroxide (H_2O_2) was found to serve as an oxidizing etchant, which induces the formation of planar twinned seeds, removes possible non-twinned nuclei, and eventually produces silver nanoplates with high yields (Chen et al., 2015; Yu et al., 2014). H_2O_2 is well-known as an effective corrosive (a strong oxidizing agent). So, it is used to dissolve silver metal because the potential of the peroxide-water pair depends on the pH value in both conditions (acid, alkaline solution) and is higher than the potential of Ag^+/Ag ($E^0 = 0.7996$ V) (Zhang et al., 2011).

In acidic solutions:

$$H_2O_2 + 2H^+ + 2e^- \rightarrow 2H_2O \quad E^0 = 1.763\ \text{V}\ (1)$$

and in alkaline solutions:

$$H_2O_2 + 2e^- \rightarrow 2OH^- \quad E^0 = 0.867\ \text{V}\ (2)$$

In this AgNP synthesis process, the volume of H_2O_2 30% ranging from 0 to 60 μL was explored to investigate the role of H_2O_2 in forming silver nanoplates. With the volume of H_2O_2 from 30 μL to 60 μL, three SPR bands appeared in the UV-Vis spectrum: (I) a small band at 322-349 nm, (II) a shoulder band around 450 nm, (III) a strong absorption band at 550-800 nm were assigned to out-of-plane quadrupole resonance, in-plane quadrupole resonance, and in-plane dipole plasmon resonance of silver nanoplates (Amirjani et al., 2020; Amirjani et al., 2019). The (III) peak underwent the red-shift from 532 nm to 739 nm **(see Figure. 1)**, corresponding to the increase in the volume of H_2O_2 from 30 to 50 μL, indicating that there is a shaped transition from silver nanodisks to hexagonal nanoplate to triangular silver nanoplates (Amirjani et al., 2019). However, in sample with larger volumes of H_2O_2 (60 μL), this wavelength tends to blueshift from 739 to 689 nm, suggesting that the excess of H_2O_2 existed in the reaction solution leads to instability of silver nanotriangles because their shape tips with high surface energy were easily etched compared to other shapes. On the other hand, a sample prepared without H_2O_2 exhibited only the formation of spherical silver nanoparticles, characterized by SPR peak at 400 nm. A small volume of H_2O_2 (10 μL) was added into the reaction mixture leading to a redshift in the UV-Vis curve. The UV spectrum performed three unclear absorption bands when the volume of H_2O_2 was increased to 20 μL. The SEM image of the 10 μL sample (Figure. 4a-(A-1)) reveals the formations of polydisperse which the size of AgNPls approximately is 106 nm (**see Figure. 4d**). These results help assert the essential role of H_2O_2 in forming silver nanoplates in this synthesis process. The appropriate volume of H_2O_2 that can be achieved through this investigation is 50 μL, which is used in further experiments. Because the peak of the 50 μL of H_2O_2 solution sample shifts toward red-shift wavelengths compared to other solution surveys. Besides, SEM image shows that the triangular peaks of the volume is 50 μL H_2O_2 are sharper than other samples.

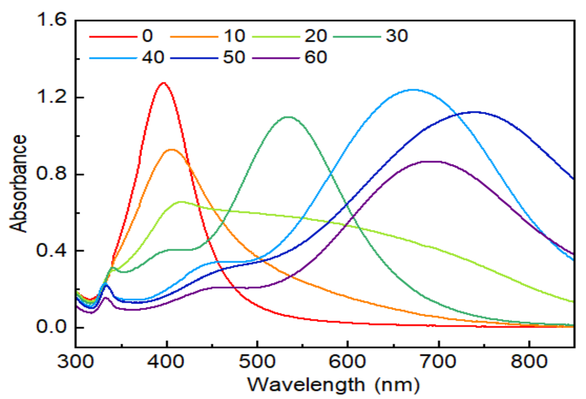

Figure 1. UV-Vis spectra of AgNPls colloidal solutions prepared with different volumes of 30% H_2O_2 ranging from 0 to 60 μL.

3.2. Effect of $NaBH_4$ volume on the formation of AgNPls.

The effect of $NaBH_4$ reagent in the synthesis of AgNPls was also examined in this process. $NaBH_4$ was considered as a strong reducing agent, which reduced most metal ions to metal atoms (Ajitha et al., 2016; Mirzaei et al., 2017). The chemical reaction of reducing $AgNO_3$ in the presence of $NaBH_4$ was described as follows:

$$2AgNO_3 + 2NaBH_4 \rightarrow 2Ag + B_2H_6 + 2NaNO_3 + H_2\uparrow \quad (3)$$

$NaBH_4$ is well-known as a reducing agent, it was also found to have a secondary role as a capping agent that can stabilize Ag nanoparticles, as evidenced by nucleation at high- concentrations of $NaBH_4$ occurring over more extended periods (Huang et al., 2008; Yi et al., 2012).

Here, we design the experiment by changing the volume of NaBH4 added to the solution from 100 to 250 µL with the remaining other factors unchanged (parameters see in Table 1). In samples prepared with $NaBH_4$ sequence 100, 125, and 150 µL volume, the UV-Vis spectra have broader SPR bands, making distinguishing three separated peaks of silver nanoplates difficult. The SEM image of the 100 µL sample **(Figure. 4b-(B-1)**) reveals the formations of polydispersed silver nanoparticles, including spheres and nanodisks. When the volume of $NaBH_4$ was increased to 175 and 200 µL, the spectra curve red-shifted of the (III) absorption band from 705 to 774 nm **(see Figure. 2)**, which is due to the in-plane dipole plasmon resonance. That change is susceptible to nanoparticles size and aspect ratio. The size of AgNPls of sample with 200 µL of $NaBH_4$ approximately 74 nm. **(see Figure. 4e)**. However, we also noticed that as the volume of $NaBH_4$ was further increased, the LSPR band tended to blue-shift from 730 nm (225 µL) to 709 nm (250 µL). The relatively broad peak implies a broad size distribution of the Ag nanoplates, consistent with the SEM characterization **(see Figure. 4b-(B-3)).** These experiments showed that 200 µL of $NaBH_4$ is the appropriate volume in this synthesis condition, and it can be used for subsequent investigations.

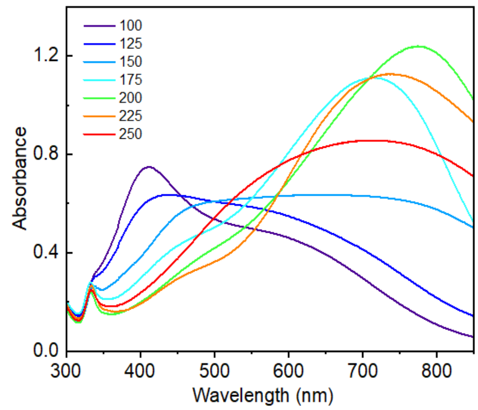

Figure 2. UV-Vis spectra of AgNPls colloidal solutions prepared with various $NaBH_4$ (0.1 M) volumes ranging from 100 to 250 µL

3.3. Effect of TSC concentration on the formation of AgNPls.

It was supposed that trisodium citrate (TSC) plays an important role in metal nanoparticle synthesis, particularly Au, Ag, and Cu, serving as a stabilizing and shape direction (Dang et al., 2015; Roh et al., 2010; Velgosova et al., 2022; Zhang et al., 2011). The different TSC concentrations ranging from 0.025 M to 0.125 M were investigated and the UV-Vis results were shown in **Figure. 3.** At the same time, other factors remained unchanged (see Table 1).

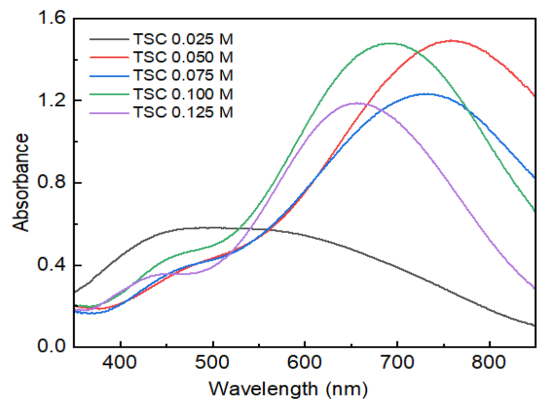

Figure 3. UV-Vis spectra of AgNPls colloidal solutions prepared with various concentrations of TSC ranging from 0.025 M

The UV-Vis spectrum of the 0.025 M TSC sample only shows a broad peak at wavelength 504 nm, revealing that nanoparticles were formed with high polydisperse and diverse shapes. This was also confirmed by the SEM images presented below (**Figure. 4c-(C-3))**. In this case, using the low concentration of TSC could not help achieving the nanoplate structures. Next, when increasing the TSC concentration up to 0.050 M, a strong LSPR band at 759 nm can be observed, indicating the formation of AgNPls, the size of which is approximately 62 nm (**see Figure. 4f**). TSC is considered an effective stabilizer with the citrate ligands responsible for effectively preventing the overgrowth of Ag on the {111 surfaces and ensuring longitudinal anisotropic growth in the side direction (Huang et al., 2008; Zhang et al., 2011). Thus, accordant TSC concentration promotes anisotropic growth and forms silver nanotriangle structures. SEM image (**Figure. 4c-(C-2)**) confirms the high density of silver nanotriangles presence in the sample synthesized with 0.05 M TSC.

TEM were used to determine the structure of the synthesized nano; the results were consistent with the UV-Vis spectrum (in the case of 0.05 M TSC). Though TEM (**Figure. 5a**) shows that the crystal faces run parallel to the structural wall. Besides, HRTEM image **(Figure. 5b)** shows that the upper faces of the triangle are formed from the plane and the distance of the inner set of faces is 0.252 nm which is attributed to the forbidden 1/3{422} reflection; The previous report shows that the triangular nanoplate is limited by the {111} planes from the top to bottom faces and the three side {100} planes as the side faces (Yang et al., 2007). On the other hand, with further increases in TSC concentration to 0.100 M and 0.125 M TSC, respectively, the LSPR peaks of these samples tend to be blue-shift. Simultaneously, the absorbance would be decreased when compared to TSC 0.100 M, indicating higher polydispersity of AgNPl colloid. This phenomenon can be supported by SEM characterization, as shown in **Figure. 4-c** below, AgNPls are formed with an average size around 84 nm. The SEM image display morphology of silver nanoparticles synthesized with 0.1 M TSC, which tends to transform into truncated shapes of triangular nanoparticles. Consequently, these results clarify the TSC crucial role in the synthesis of silver nanoplates, primarily affecting the transformation shape of silver nanoplates.

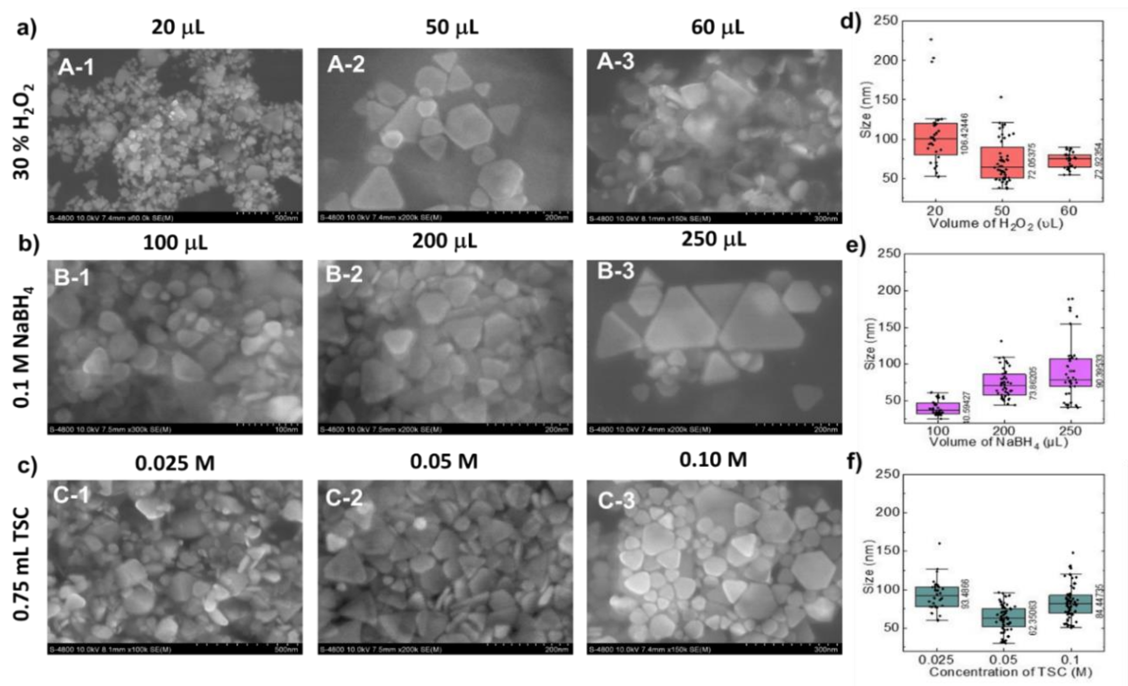

Figure 4. SEM images a) investigates the effect of volume of 30% H_2O_2 at 20, 50, 60 μL b) volume of 0.100 M $NaBH_4$ at 100, 200, 250 μL; c) concentration TSC at 0.025, 0.05, 0.100 M; d-f) box overlaps show the size distribution of AgNPls corresponding to the SEM images a, b, c.

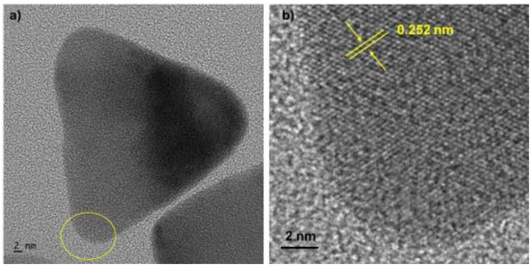

Figure 5. a) TEM images of silver nanoplates at 0.05 M of TSC, 200 μL $NaBH_4$, 50 μL H_2O_2. b) The high-resolution transmission microscopy image shows the distance of the inner set of faces is 0.252 nm.

AgNPs prepared with 0.05 M of TSC, 200 μL $NaBH_4$, 50 μL H_2O_2, and 60 μL $AgNO_3$ showed more uniformity and vicinity tips and edges. Therefore, this condition was used for further experiments to test Antibacterial activity.

3.4. Antibacterial activity of AgNPls

For investigating the effect of AgNPls, the antibacterial activity was evaluated at different concentrations against Gram-positive (*S. aureus*, *L. innocua*) and Gram-negative bacteria (*E. coli*, *P. aeruginosa*) based on the agar disk diffusion method. AgNPls showed antibacterial activity at lowest concentration (0.625 μg/mL) for *S. aureus* bacteria strain. For *L. innocua* bacteria strains, AgNPs displayed antibacterial activity at AgNPls concentration of 1.25 μg/mL, and it was increased to 2.5 μg/mL for *E. coli*, *P. aeruginosa* bacteria strains (**see in Figure. 6& Figure. 7**). These results showed that silver nanoplates present antibacterial activity against gram-positive bacteria at low concentrations better than that against gram-negative bacteria. It is probably because Gram-positive and Gram-negative bacteria differ in cell walls. The cell walls of gram-negative bacteria include polysaccharides (LPS) which do not exist in gram-positive bacteria, providing effective protection against biocides(Steimle et al., 2016).

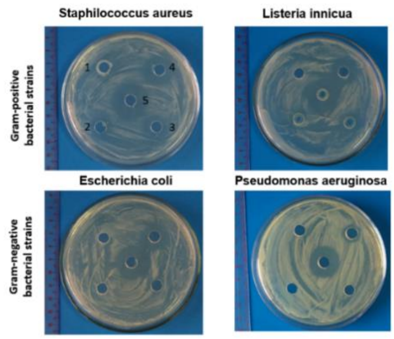

Figure 6. Anti-microbial activity of silver nanoplates showing clear zones at different concentrations (1) 0.3125, (2) 0.625, (3) 1.25, (4) 2.5, (5) 5 μg/mL inhibition against *Staphylococcus aureus*, *Listeria innocua*, *Escherichia coli*, and *Pseudomonas aeruginosa.*

Table 2. Inhibitor diameter at different concentrations of silver nanoplate against *S. aureus*, *L. innocua*, *E. coli*, and *P. aeruginosa*.

Bacterial strains	**Antimicrobial diameter (mm) at different concentrations of silver nanoplates (μg/mL)**				
	0.3125	**0.625**	**1.25**	**2.5**	**5**
S. aureus (+)	$0,00^{e}\pm0,00$	$\mathbf{3,83^{d}\pm0,29}$	$5,57^{c}\pm0,06$	$8,77^{b}\pm0,25$	$15,67^{a}\pm0,29$
L. innocua (+)	$0,00^{d}\pm0,00$	$0,00^{d}\pm0,00$	$\mathbf{4,17^{c}\pm0,29}$	$9,07^{b}\pm0,12$	$13,17^{a}\pm0,76$
E. coli (-)	$0,00^{c}\pm0,00$	$0,00^{c}\pm0,00$	$0,00^{c}\pm0,00$	$\mathbf{9,07^{b}\pm0,12}$	$12,80^{a}\pm0,53$
P. aeruginosa (-)	$0,00^{c}\pm0,00$	$0,00^{c}\pm0,00$	$0,00^{c}\pm0,00$	$\mathbf{5,30^{b}\pm0,27}$	$12,33^{a}\pm0,58$

Note: Values followed by the same letter in the same row are not statistically different ($p>0.05$).

Additionally, we found that the antibacterial activity increased when we increased the concentration of silver nanoplates. Particularly, the antimicrobial diameter against *S. aureus* increases from 3,83^{d}±0,29 to 15,67^{a}±0,29 when AgNPl concentration increases from 0.625 to 5 µg/mL, respectively (**see in Figure. 7**). This trend is the same for other bacterial strains in the bacterial test. Through these results, we can see the relationship between the concentration and antibacterial effect of silver nanoplates. On the other hand, at the higher concentrations of 5 µg/mL, AgNPls showed similar antibacterial activity against both gram-positive and gram-negative bacteria. This phenomenon is confirmed by the antimicrobial diameter for *S. aureus, L. innocua*, *E. Coli*, and *P. aeruginosa* as 15,67^{a}±0,29, 13,17^{a}±0,76, 12,80^{a}±0,53, 12,33^{a}±0,58, respectively (**see in Figure. 7**). The previous studies concluded that gram-positive bacteria's cell wall (10-80 nm) (Rohde, 2019) is significantly thicker than that of gram-negative bacteria (2-8 nm) (Huang et al., 2008; Matias et al., 2005). However, the antibacterial activity of AgNPls was shown to not be affected too much by differences in bacterial cell walls at higher concentrations.

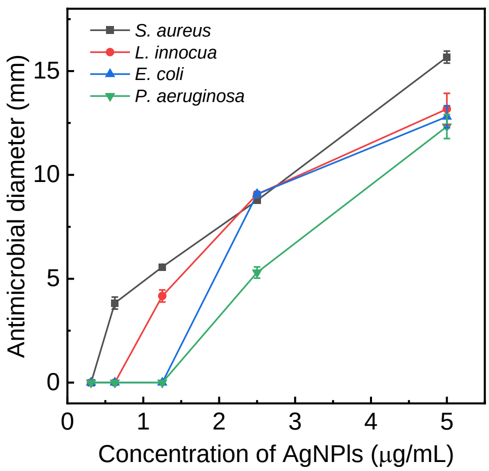

Figure 7. Inhibitor diameter at different concentrations of silver nanoplate against *S. aureus, L. innocua, E. coli,* and *P. aeruginosa*.

According to the antibacterial mechanism of Ag nanoparticles, it shows that Ag nanoparticles are oxidized to form Ag+ ions that easily penetrate cell membranes, leading to cell death by destroying protein structures (Djafari et al., 2019). Besides, the previous studies concluded that Gram-positive bacteria's cell wall (10-80 nm) (Rohde, 2019) is significantly thicker than that of Gram-negative bacteria (2-8 nm) (Huang et al., 2008; Matias et al., 2005) while research results show that at high concentrations specifically 5 µg/mL, we found that the antimicrobial diameter of Gram-positive lager than Gram-negative bacteria such as the antimicrobial diameter of *E. coli* and *P. aeruginosa* sequence are 12,80a±0,53 and 12,33a±0,58 while the antimicrobial diameter of *S. aureus* and *L. innocua* are 15,67a±0,29 and 13,17a±0,76. The result shows that the cell membranes are not effectively too much ability antibacterial activity of silver nanoplates.

4. CONCLUSION

In this study, we have successfully synthesized AgNPls with a facile single step synthesis. Besides, this study evaluates the effects of parameters such as H_2O_2, $NaBH_4$, and TSC in this synthesized process to obtain shape AgNPls and a higher amount of nanoplates in the reaction solution. These reagents play a crucial role in tuning the nanoplate shape, as well as the thickness and edge length of the AgNPls. Moreover, we have discovered the antibacterial ability of prepared silver nanotriangles against Gram-positive such as *Staphylococcus aureus*, *Listeria innocua* and Gram-negative bacteria such as *Escherichia coli, Pseudomonas aeruginosa*, at low concentrations (2.5 µg/mL). We found that the prepared AgNPls against gram-positive bacteria are at a lower concentration (0.3215 µg/mL for *S. aureus*) than that of gram-negative bacteria and do not depend too much on the thickness of the bacterial cell wall at an appropriate concentration. That shows silver nanoplates are an ideal material for future antibacterial applications.

ACKNOWLEDGEMENT

We appreciate the invaluable analysis method supported by the Research Institute of Clean Manufacturing System, Korea Institute of Industrial Technology (KITECH), and KITECH school, University of Science and Technology (UST). We also grateful for analytical support from Central Laboratory for Analysis, University of Science, Vietnam National University Ho Chi Minh City, Vietnam.

REFERENCES

Agnihotri, S., Mukherji, S., & Mukherji, S. (2014). Size-controlled silver nanoparticles synthesized over the range 5–100 nm using the same protocol and their antibacterial efficacy. *RSC Advances*, *4*(8), 3974-3983. doi:10.1039/C3RA44507K

Ajitha, B., Reddy, Y. A. K., Kim, M. J., Jeon, H.-J., & Ahn, C. W. (2016). Superior catalytic activity of synthesized triangular silver nanoplates with optimized sizes and shapes. *Catalysis Science & Technology*, *6*(23), 8289-8299. doi:10.1039/C6CY01948J

Amirjani, A., Firouzi, F., & Haghshenas, D. F. (2020). Predicting the Size of Silver Nanoparticles from Their Optical Properties. *Plasmonics, 15*(4), 1077-1082. doi:10.1007/s11468-020-01121-x

Amirjani, A., Koochak, N. N., & Haghshenas, D. F. (2019). Synthesis of silver nanotriangles with tunable edge length: a promising candidate for light harvesting purposes within visible and near–infrared ranges. *Materials Research Express*, *6*(3), 036204. doi:10.1088/2053-1591/aaf624

Anees Ahmad, S., Sachi Das, S., Khatoon, A., Tahir Ansari, M., Afzal, M., Saquib Hasnain, M., & Kumar Nayak, A. (2020). Bactericidal activity of silver nanoparticles: A mechanistic review. *Materials Science for Energy Technologies, 3*, 756-769. doi:10.1016/j.mset.2020.09.002

Chen, Z., Zhang, C., Wu, Q., Li, K., & Tan, L. (2015). Application of triangular silver nanoplates for colorimetric detection of H2O2. *Sensors and Actuators B: Chemical, 220*, 314-317. doi:10.1016/j.snb.2015.05.085

Cheon, J. Y., Kim, S. J., Rhee, Y. H., Kwon, O. H., & Park, W. H. (2019). Shape-dependent antimicrobial activities of silver nanoparticles. *Int J Nanomedicine, 14*, 2773-2780. doi:10.2147/ijn.S196472

Dakal, T. C., Kumar, A., Majumdar, R. S., & Yadav, V. (2016). Mechanistic Basis of Antimicrobial Actions of Silver Nanoparticles. *7*. doi:10.3389/fmicb.2016.01831

Dang, D. M. T., Dang, C. M., & Fribourg–Blanc, E. (2015). Study of the formation of silver nanoparticles and silver nanoplates by chemical reduction method. *International Journal of Nanotechnology*, *12*(5-7), 456-465. doi:10.1504/IJNT.2015.067903

Djafari, J., Fernández-Lodeiro, C., Fernández-Lodeiro, A., Silva, V., Poeta, P., Igrejas, G., Fernández-Lodeiro, J. (2019). Exploring the Control in Antibacterial Activity of Silver Triangular Nanoplates by Surface Coating Modulation. *6*. doi:10.3389/fchem.2018.00677

Dong, Y., Zhu, H., Shen, Y., Zhang, W., & Zhang, L. (2019). Antibacterial activity of silver nanoparticles of different particle size against Vibrio Natriegens. *PLoS One, 14*(9), e0222322. doi:10.1371/journal.pone.0222322

Fu, J., Ji, J., Fan, D., & Shen, J. (2006). Construction of antibacterial multilayer films containing nanosilver via layer-by-layer assembly of heparin and chitosan-silver ions complex. *J Biomed Mater Res A, 79*(3), 665-674. doi:10.1002/jbm.a.30819

Furletov, A. A., Apyari, V. V., Zaytsev, V. D., Sarkisyan, A. O., & Dmitrienko, S. G. (2023). Silver triangular nanoplates: Synthesis and application as an analytical reagent in optical molecular spectroscopy. A review. *TrAC Trends in Analytical Chemistry, 166*, 117202. doi:10.1016/j.trac.2023.117202

Gao, M., Sun, L., Wang, Z., & Zhao, Y. (2013). Controlled synthesis of Ag nanoparticles with different morphologies and their antibacterial properties. *Materials Science and Engineering: C, 33*(1), 397-404. doi:10.1016/j.msec.2012.09.005

Guzman, M., Dille, J., & Godet, S. (2012). Synthesis and antibacterial activity of silver nanoparticles against gram-positive and gram-negative bacteria. *Nanomedicine: Nanotechnology, Biology and Medicine, 8*(1), 37-45. doi:10.1016/j.nano.2011.05.007

Huang, K. C., Mukhopadhyay, R., Wen, B., Gitai, Z., & Wingreen, N. S. (2008). Cell shape and cell-wall organization in Gram-negative bacteria. *Proc Natl Acad Sci U S A, 105*(49), 19282-19287. doi:10.1073/pnas.0805309105

Lu, W., Yao, K., Wang, J., & Yuan, J. (2015). Ionic liquids–water interfacial preparation of triangular Ag nanoplates and their shape-dependent antibacterial activity. *J Colloid Interface Sci, 437*, 35-41. doi:10.1016/j.jcis.2014.09.001

Matias, V. R., & Beveridge, T. J. (2005). Cryo-electron microscopy reveals native polymeric cell wall structure in Bacillus subtilis 168 and the existence of a periplasmic space. *Mol Microbiol, 56*(1), 240-251. doi:10.1111/j.1365-2958.2005.04535.x

Mirzaei, A., Janghorban, K., Hashemi, B., Bonyani, M., Leonardi, S. G., & Neri, G. (2017). Characterization and optical studies of PVP-capped silver nanoparticles. *Journal of Nanostructure in Chemistry, 7*(1), 37-46. doi:10.1007/s40097-016-0212-3

Munro, C. H., Smith, W. E., Garner, M., Clarkson, J., & White, P. C. (1995). Characterization of the Surface of a Citrate-Reduced Colloid Optimized for Use as a Substrate for Surface-Enhanced Resonance Raman Scattering. *Langmuir, 11*(10), 3712-3720. doi:10.1021/la00010a021

Pastoriza-Santos, I., & Liz-Marzán, L. M. (2008). Colloidal silver nanoplates. State of the art and future challenges. *Journal of Materials Chemistry, 18*(15), 1724-1737. doi:10.1039/B716538B

Roh, J., Park, E.-J., Park, K., Yi, J., & Kim, Y. (2010). Fast preparation of citrate-stabilized silver nanoplates and its nanotoxicity. *Korean Journal of Chemical Engineering, 27*(6), 1897-1900. doi:10.1007/s11814-010-0299-z

Rohde, M. (2019). The Gram-Positive Bacterial Cell Wall. *Microbiology Spectrum, 7*(3), 10.1128/microbiolspec.gpp1123-0044-2018. doi:10.1128/microbiolspec.gpp3-0044-2018

Saubolle, M. A., & Hoeprich, P. D. (1978). Disk agar diffusion susceptibility testing of yeasts. *Antimicrob Agents Chemother, 14*(4), 517-530. doi:10.1128/aac.14.4.517

Sotiriou, G. A., Meyer, A., Knijnenburg, J. T. N., Panke, S., & Pratsinis, S. E. (2012). Quantifying the Origin of Released Ag^+ Ions from Nanosilver. *Langmuir, 28*(45), 15929-15936. doi:10.1021/la303370d

Steimle, A., Autenrieth, I. B., & Frick, J. S. (2016). Structure and function: Lipid A modifications in commensals and pathogens. *Int J Med Microbiol, 306*(5), 290-301. doi:10.1016/j.ijmm.2016.03.001

Velgosova, O., Mačák, L., Čižmárová, E., & Mára, V. (2022). Influence of Reagents on the Synthesis Process and Shape of Silver Nanoparticles. *Materials, 15*(19). doi:10.3390/ma15196829

Yang, Y., Matsubara, S., Xiong, L., Hayakawa, T., & Nogami, M. (2007). Solvothermal Synthesis of Multiple Shapes of Silver Nanoparticles and Their SERS Properties. *The Journal of Physical Chemistry C, 111*(26), 9095-9104. doi:10.1021/jp068859b

Yi, Z., Zhang, J.-b., He, H., Xu, X.-b., Luo, B.-c., Li, X.-b., . . . Yi, Y.-g. (2012). Convenient synthesis of silver nanoplates with adjustable size through seed mediated growth approach. *Transactions of Nonferrous Metals Society of China, 22*(4), 865-872. doi:10.1016/S1003-6326(11)61258-2

Yu, H., Zhang, Q., Liu, H., Dahl, M., Joo, J. B., Li, N., . . . Yin, Y. (2014). Thermal Synthesis of Silver Nanoplates Revisited: A Modified Photochemical Process. *ACS Nano, 8*(10), 10252-10261. doi:10.1021/nn503459q

Zannotti, M., Vicomandi, V., Rossi, A., Minicucci, M., Ferraro, S., Petetta, L., & Giovannetti, R. (2020). Tuning of hydrogen peroxide etching during the synthesis of silver nanoparticles. An application of triangular nanoplates as plasmon sensors for Hg^{2+} in aqueous solution. *Journal of Molecular Liquids, 309*, 113238. doi:10.1016/j.molliq.2020.113238

Zhang, Q., Li, N., Goebl, J., Lu, Z., & Yin, Y. (2011). A Systematic Study of the Synthesis of Silver Nanoplates: Is Citrate a “Magic” Reagent? *J Am Chem Soc, 133*(46), 18931-18939. doi:10.1021/ja2080345

TỔNG HỢP NANO BẠC DẠNG PHIẾN ỨNG DỤNG KHÁNG KHUẨN

Trịnh Như Bảo[1,2], Nguyễn Anh Thư[1,2], Phan Thị Ngọc Cẩm[1,2], Trương Tấn Trung[3], Võ Quốc Khương[1,2*].

[1]Trường Đại học Khoa học Tự nhiên, Đại học Quốc gia Thành phố Hồ Chí Minh
[2]Đại học Quốc gia Thành Phố Hồ Chí Minh
[3]Trường Đại học Công nghệ Đồng Nai
**Tác giả liên hệ: Võ Quốc Khương, vqkhuong@hcmus.edu.vn*

THÔNG TIN CHUNG

Ngày nhận bài: 14/12/2023

Ngày nhận bài sửa: 02/03/2024

Ngày duyệt đăng: 12/03/2024

TỪ KHOÁ

Hoạt tính kháng khuẩn của các phiến nano bạc;

Phiến nano bạc.

TÓM TẮT

Các phiến nano bạc (AgNPls) rất hấp dẫn nhờ các đặc tính độc đáo của chúng, bao gồm cộng hưởng plasmon bề mặt cục bộ (LSPR) và khả năng kháng khuẩn nhờ các đầu và cạnh của chúng. Nghiên cứu này báo cáo một phương pháp nhanh chóng và đơn giản để điều chế các phiến nano bạc bằng cách sử dụng phương pháp tổng hợp một bước với sự có mặt của tiền chất $AgNO_3$, $NaBH_4$, TSC và tác nhân oxy hóa H_2O_2. Việc điều chỉnh tỷ lệ tiền chất có thể mang lại nhiều hình thái khác nhau như hình cầu, đĩa nano, cấu trúc lục giác và phiến nano hình tam giác, mỗi hình dạng thể hiện LSPR khác nhau. Các đặc tính quang học của AgNPls được phân tích bằng phương pháp quang phổ UV-Vis và phân tích hình thái bằng SEM. Phân tích các cấu trúc tinh thể đặc trưng bởi TEM và HR-TEM. Hơn nữa, hoạt tính kháng khuẩn cũng được đánh giá chống lại 04 chủng vi khuẩn, bao gồm *Staphylococcus aureus, Listeria innocua, Escherichia coli* và *Pseudomonas aeruginosa*. AgNPls được điều chế trong nghiên cứu này cho thấy hoạt tính kháng khuẩn chống lại vi khuẩn gram dương tốt hơn ở nồng độ thấp (0,625 µg/mL) so với vi khuẩn gram âm. Kết quả thể hiện hoạt tính kháng khuẩn không phụ thuộc quá nhiều vào độ dày thành tế bào vi khuẩn ở nồng độ thấp.